

**Cell Reports, Volume 44**

**Supplemental information**

**A direct interaction between the RNA-binding  
proteins Staufen and Tm1-I/C  
in the *oskar* mRNA transport complex**

**Thomas Gaber, Thomas Monecke, Julia Grabowski, Bernd Simon, Tobias Williams, Vera Roman, Jeffrey Chao, Janosch Hennig, Anne Ephrussi, Dierk Niessing, and Simone Heber**

## Supplementary data

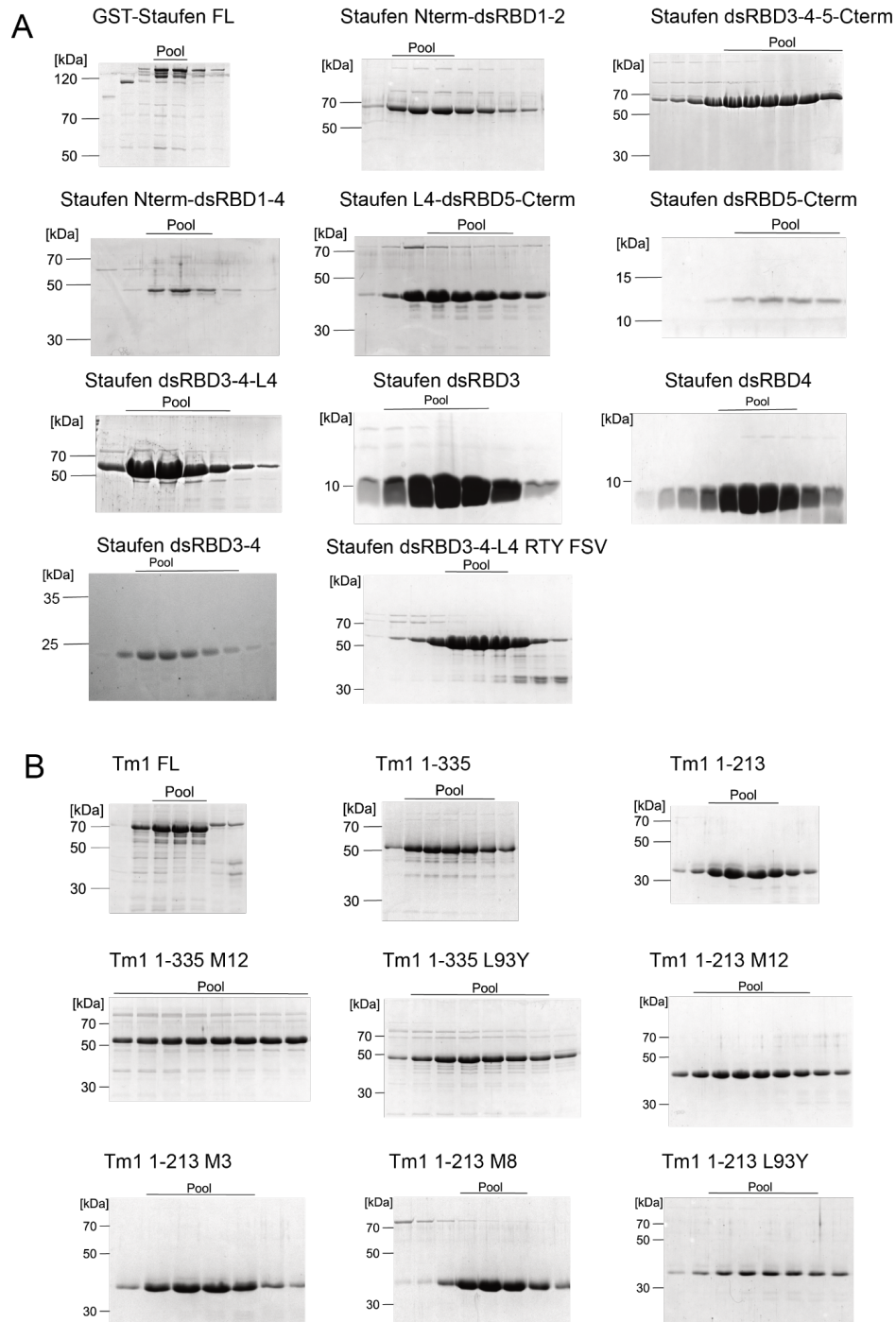


**Figure S1: Purified Staufen and Tm1 proteins used in this study, related to Figures 1, 2, 3, 4. A)** Exemplary SDS-PAGE of final size exclusion chromatography purification step for all used Staufen proteins and **B)** for all used Tm1 proteins. Fractions pooled for subsequent experiments are indicated.

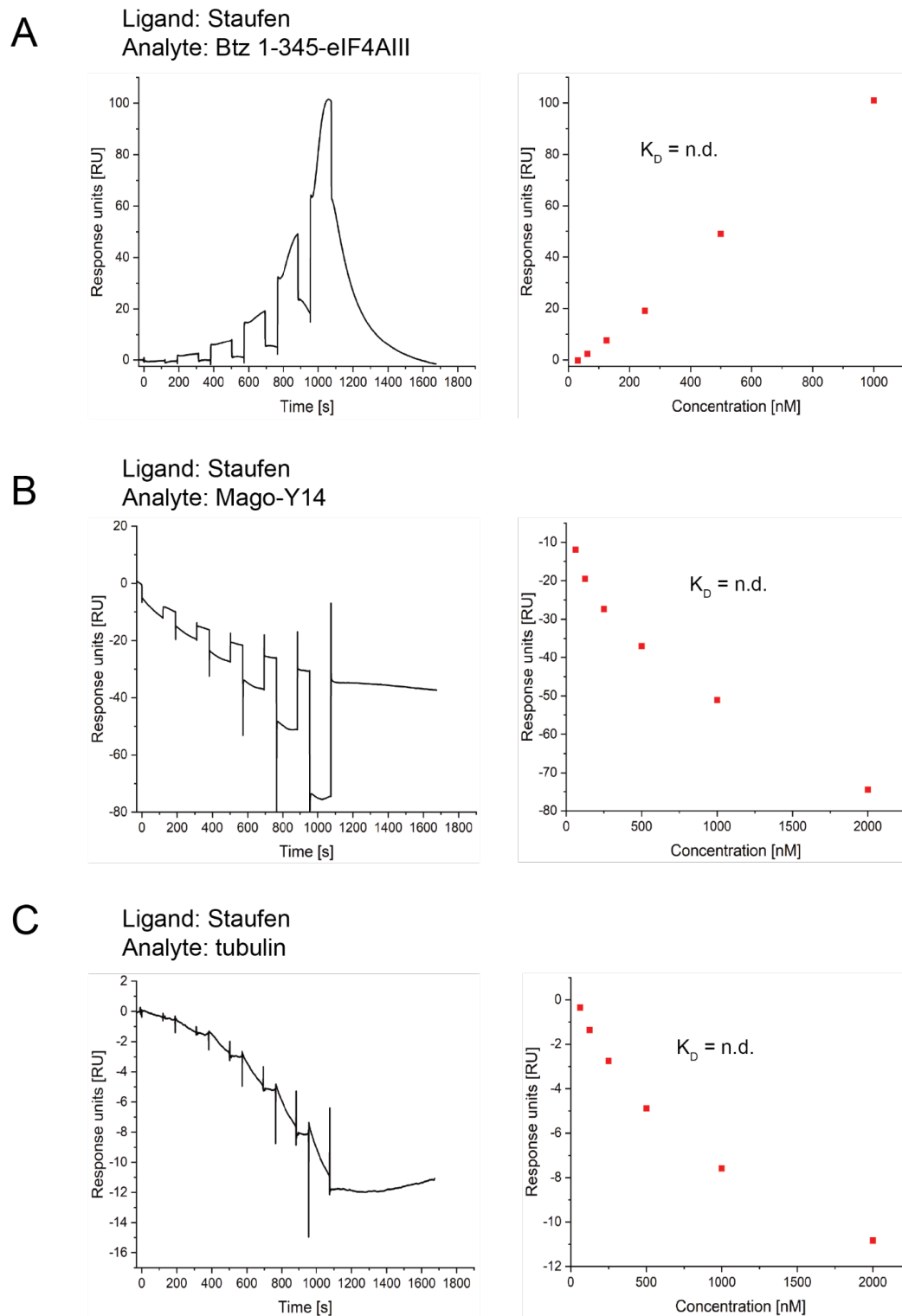
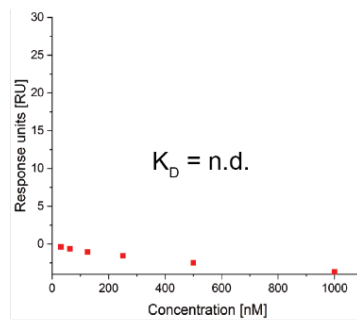
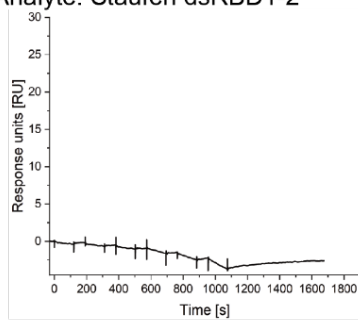
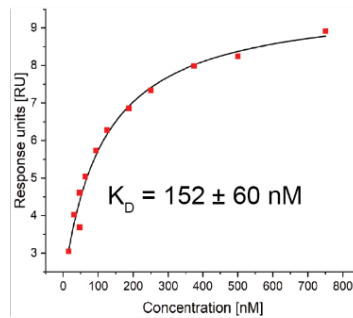
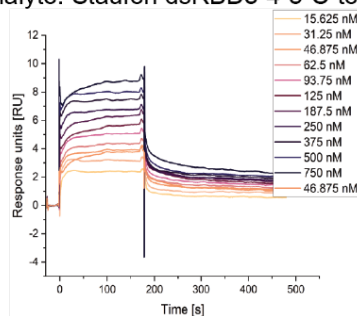


**Figure S2: In SPR no interaction between Staufen and EJC components or tubulin are detected, related to Figure 1. A-C) Single-cycle experiment sensorgrams and response concentration plot for Btz SELOR-eIF4AIII (A), Mago-Y14 (B) and tubulin (C) injected onto surface coupled Staufen FL. Due to a lack of concentration-dependent saturation, no equilibrium dissociation constants ( $K_D$ ) could be determined.**

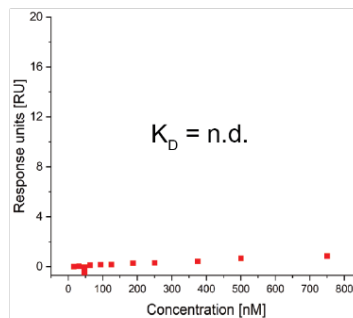
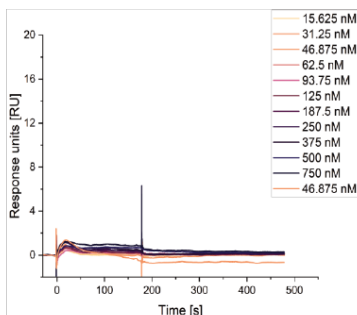
**A** Ligand: Tm1 FL  
Analyte: Staufen dsRBD1-2



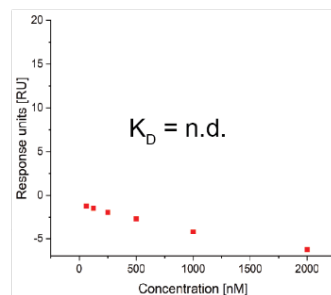
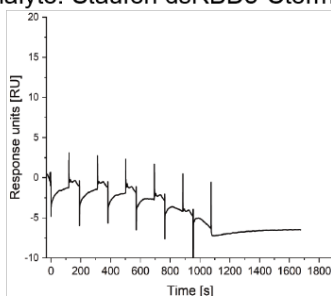
**B** Ligand: Tm1 FL  
Analyte: Staufen dsRBD3-4-5-C-term



**C** Ligand: Tm1 FL  
Analyte: Staufen dsRBD1-4



**D** Ligand: Tm1 FL  
Analyte: Staufen dsRBD5-Cterm



**E** Ligand: Tm1 FL  
Analyte: Staufen L4-dsRBD5-Cterm

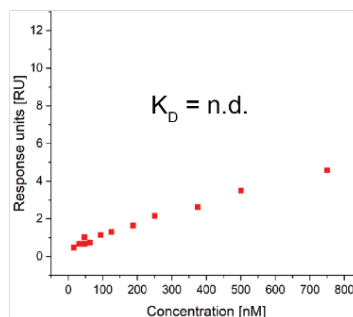
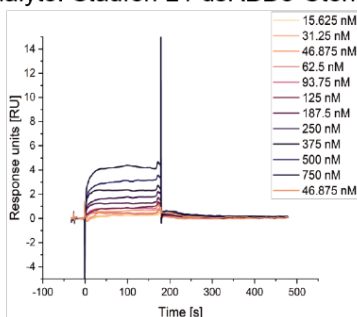


**Figure S3: Staufen fragments showing no binding to Tm1 FL, related to Figure 2. A-E)** Sensorgrams (left) and response concentration plots (right) of SPR experiments with Staufen dsRBD1-2 (A), Staufen dsRBD3-4-5-C-term (B), Staufen dsRBD1-4 (C), Staufen dsRBD5-Cterm (D) and Staufen L4-dsRBD5-Cterm (E) show no concentration-dependent saturation of binding to surface-coupled Tm1 FL.  $K_D$ s for Staufen dsRBD3-4-5-C-term was determined using a one-site-binding fit to the maximal response at equilibrium for each analyte concentration. The  $K_D$ -value is given as mean  $\pm$  SD from triplicate experiments. For other Staufen proteins,  $K_D$ s could not be determined.

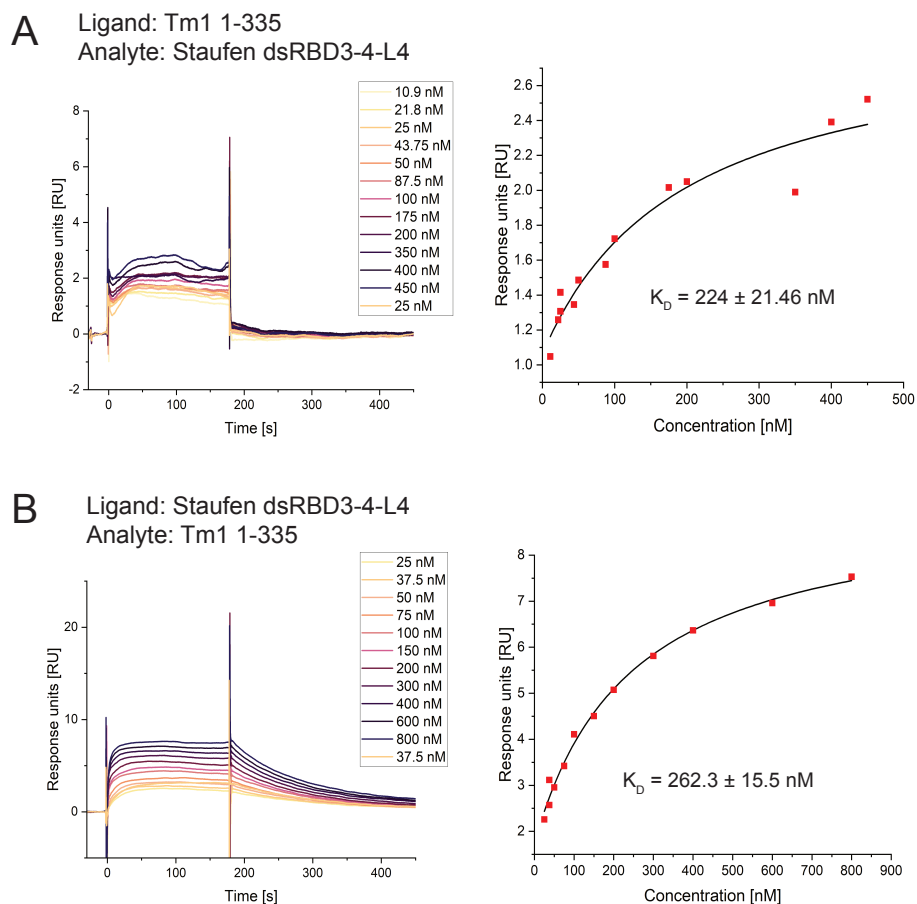


**Figure S4: In SPR experiments an interaction between Staufen dsRBD3-4-L4 and Tm1 1-335 is observed, related to Figure 2. A-B)** Multi-cycle SPR experiments show binding of Staufen dsRBD3-4-L4 to surface-coupled Tm1 1-335 (A) and Tm1 1-335 to surface-coupled Staufen dsRBD3-4-L4 (B). The overlaid sensorgrams of multi-cycle SPR experiments (left) show that binding occurs transiently.  $K_D$  was determined using a one-site-binding fit to the maximal response at equilibrium for each analyte concentration (right). The  $K_D$ -values are given as mean  $\pm$  SD from triplicate experiments.

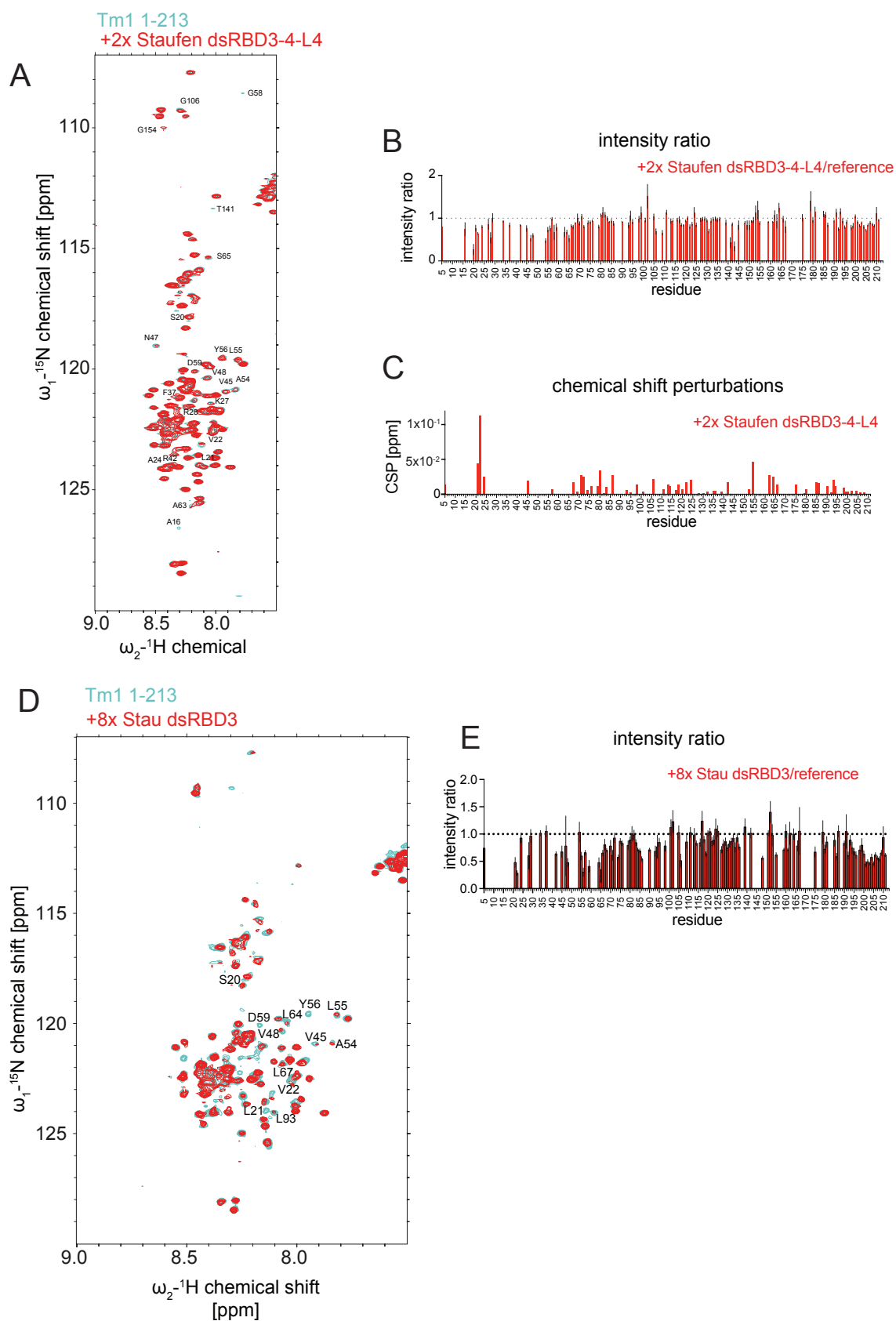


**Figure S5:**  $^1\text{H}$ - $^{15}\text{N}$  HSQC titration experiments with Tm1 1-213 and Staufen dsRBD3-4-L4 or Staufen dsRBD3, related to Figure 2. **A)**  $^1\text{H}$ - $^{15}\text{N}$  HSQC spectrum of Tm1 1-213 with backbone

assignments [S1] indicated (blue), overlaid with its  $^1\text{H}$ - $^{15}\text{N}$  HSQC spectrum after titration with a 2-fold excess of Staufén dsRBD3-4. **B)** Plotted intensity ratios and **C)** chemical shift perturbation (CSP) plot of individual residues in the titration experiment. 0.5x, 1x, 1.5x, and 2x excess Staufén dsRBD3-4-L4 was titrated to Tm1-213. 2x Staufén dsRBD3-4-L4 was the highest achievable excess. **D)**  $^1\text{H}$ - $^{15}\text{N}$  HSQC spectrum of Tm1 1-213 with backbone assignments indicated (cyan), overlaid with its  $^1\text{H}$ - $^{15}\text{N}$  HSQC spectrum after titration with an 8-fold excess of Staufén dsRBD3 (red). **E)** Plotted intensity ratios of individual residues in the titration experiment. 0.5x, 1x, 1.5x, 2x, 4x and 8x excess Staufén dsRBD3 was titrated to Tm1-213, 8x Staufén dsRBD3 was the highest achievable excess, the endpoint of the titration could not be reached.

Data are presented as measured value  $\pm$  SD. Error bars represent estimates of propagated measurement errors of the experimental uncertainties in signal amplitudes.



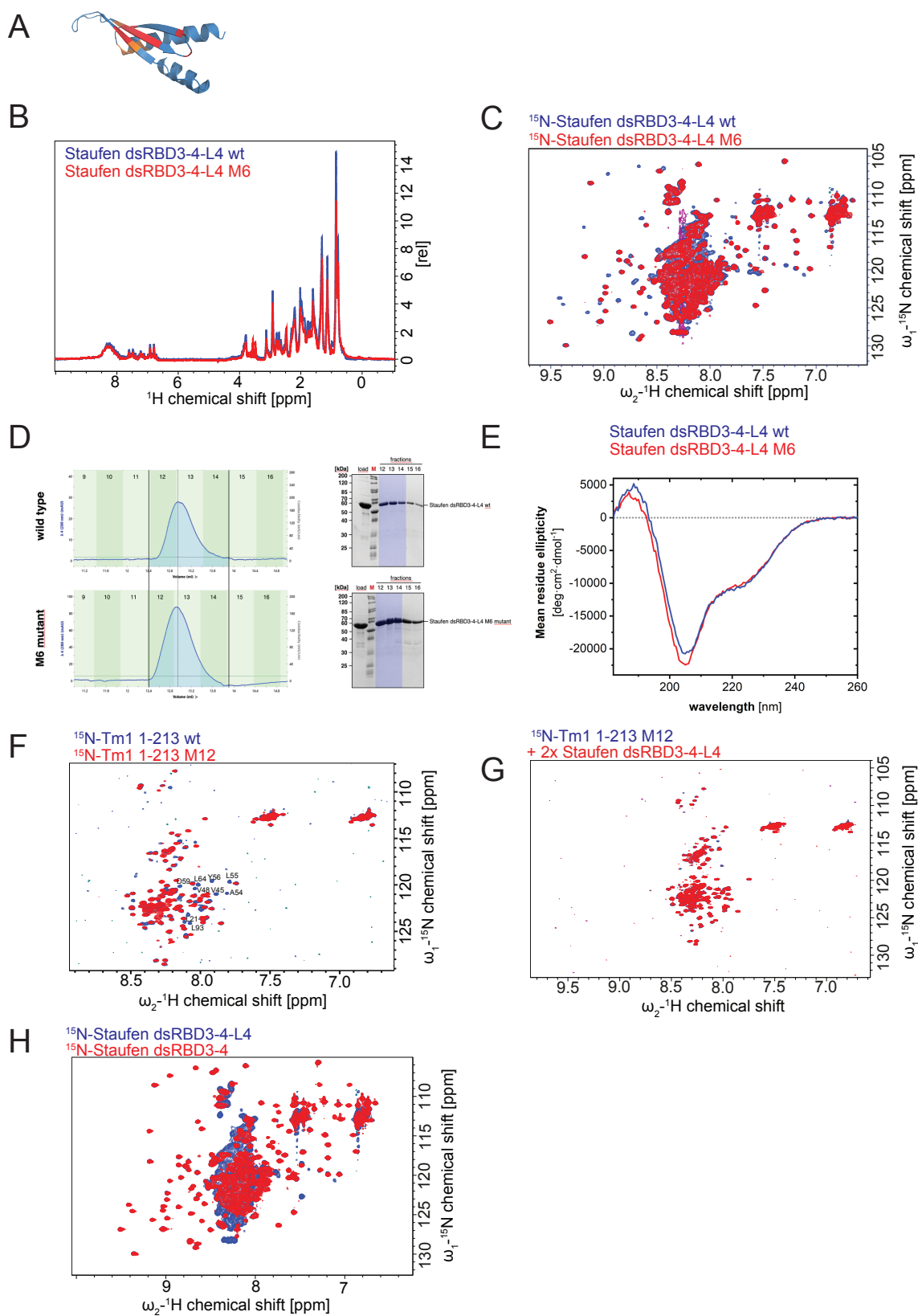


**Figure S6: Characterization of mutant proteins and protein truncations, related to Figure 3 and STAR Methods.** **A)** AlphaFold2 [S2] prediction of the Staufen dsRBD4 structure with RNA-binding residues marked in orange and Tm1-binding residues marked in red. **B-C)** Overlay of 1D (A) and  $^1\text{H}$ - $^{15}\text{N}$  HSQC (B) spectra of Staufen dsRBD3-4-L4 WT (blue) and the mutant M6 (red). **D)** Size exclusion chromatography profiles and SDS-PAGE analysis of wildtype Staufen dsRBD3-4-L4 and the M6 mutant. **E)** CD spectra of wild type and the M6 mutant. **F)** Overlay of  $^1\text{H}$ - $^{15}\text{N}$  HSQC spectra of Tm1 1-213 WT (blue) and the mutant M12 (red). The Staufen M6 mutant protein retains wildtype-like folding and the Tm1 M12 mutant protein remains unfolded. **G)**  $^1\text{H}$ - $^{15}\text{N}$  HSQC titration experiment with 50  $\mu\text{M}$   $^{15}\text{N}$ -labeled Tm1 1-213 and Staufen dsRBD3-4-L4 showed no changes of the Tm1 1-213 upon addition of Staufen dsRBD3-4-L4. 0.5x, 1x, 1.5x and 2x excess Staufen dsRBD3-4-L4 was titrated to Tm1-213 M12. 2x Staufen dsRBD3-4-L4 was the highest achievable excess. **H)**  $^1\text{H}$ - $^{15}\text{N}$  HSQC spectrum of Staufen dsRBD3-4-L4 (blue), overlaid with the  $^1\text{H}$ - $^{15}\text{N}$  HSQC spectrum of Staufen dsRBD3-4 (red), showing that the truncation of linker 4 does not alter the fold of Staufen dsRBDs 3 and 4.

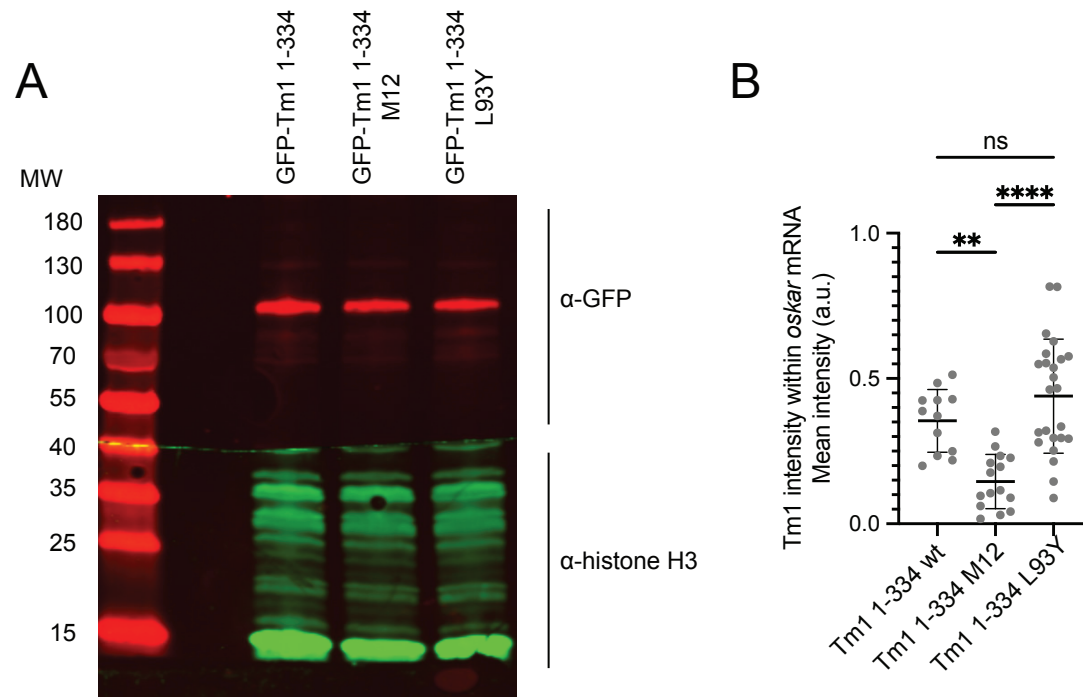


**Figure S7: Mutant Tm1 transgenic proteins are expressed to similar levels as the wildtype transgene, related to Figure 5: A)** Western blot analysis of GFP-Tm1 proteins expressed from transgenes in *Tm1[eg9]/Tm1[eg9]* *Drosophila* ovaries. All transgenes are expressed to similar levels from a UAS promoter, driven by *oskar-Gal4*. **B)** Quantification of GFP-Tm1 intensity in *oskar* mRNA-Positive regions. *oskar* mRNA was identified and segmented as a distinct object, and GFP-Tm1 intensity was quantified within these regions. The graph displays the mean GFP intensity per oocyte. Each data point represents an individual oocyte; error bars indicate mean  $\pm$  SD. Statistical significance was determined using one-way ANOVA with Dunnett's post hoc test. Statistically significant pairwise comparisons are indicated.

## Supplemental References

- S1. Vaishali, Dimitrova-Paternoga, L., Haubrich, K., Sun, M., Ephrussi, A., and Hennig, J. (2021). Validation and classification of RNA binding proteins identified by mRNA interactome capture. *RNA* 27, 1173–1185. 10.1261/rna.078700.121.
- S2. Jumper, J., Evans, R., Pritzel, A., Green, T., Figurnov, M., Ronneberger, O., Tunyasuvunakool, K., Bates, R., Žídek, A., Potapenko, A., et al. (2021). Highly accurate protein structure prediction with AlphaFold. *Nature* 596, 583–589. 10.1038/s41586-021-03819-2.